

# Adsorption of PTCDA on Terraces and at Steps Sites of the KCl(100) Surface

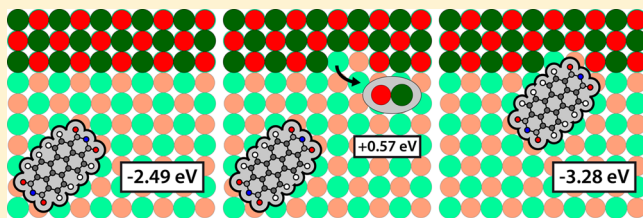
Q. Guo,<sup>†</sup> A. Paulheim, and M. Sokolowski\*

Institut für Physikalische und Theoretische Chemie der Universität Bonn, Wegelerstraße 12, D-53115 Bonn, Germany

H. Aldahhak, E. Rauls, and W. G. Schmidt

Lehrstuhl für Theoretische Physik, Universität Paderborn, Warburger Straße 100, D-33098 Paderborn, Germany

**ABSTRACT:** Scanning tunneling microscopy at low temperature and low molecular coverage ( $\sim 1\%$ ) was combined with density-functional theory calculations to investigate the adsorption of isolated perylene-3,4,9,10-tetracarboxyl acid dianhydride (PTCDA) molecules on KCl(100) surfaces. Experimentally, we used epitaxial thin KCl(100) films on Ag(100) of about 3 layers in thickness. After deposition at 100 K, the PTCDA molecules are statistically distributed on the terraces with an azimuthal orientation of the long axis along the polar  $\langle 110 \rangle$  orientation. After annealing at about 150 to 200 K the molecules are exclusively found at step-edge sites. Thereby, several configurations are observed, the most typical being a site where the PTCDA molecules protrude into the step edge, forming vacancies at the step edge. The total-energy calculations predict this step-edge adsorption site to be energetically favorable compared to the adsorption on terraces. The corrugation of the calculated potential energy surface is below 1 eV, with diffusion barriers of about 0.6 eV, which explains the mobility of the PTCDA molecules at elevated temperatures.



## 1. INTRODUCTION

The adsorption of organic molecules on insulator (dielectric) surfaces is typically dominated by electrostatic and dispersive interactions, in contrast to the covalent bond formation frequently observed for molecules adsorbed on metal surfaces.<sup>1</sup> Consequently, often only small modifications of the molecular electronic structure are induced by the surface bonding, and the intrinsic properties of functional molecules such as the molecular orbitals<sup>2</sup> or the optical response, e.g., the fluorescence<sup>3</sup> may be better preserved. This allows for studying molecular properties using sophisticated surface analysis techniques.

The adsorption of functional molecules with a nonuniform internal charge distribution on surfaces of ionic materials is particularly interesting.<sup>4,5</sup> In this case the Coulomb interactions between partial charges on functional groups of the molecule and surface anions and cations may lead to a site-specific adsorption of the molecule on the surface, possibly resulting in commensurate long-range ordered structures. In addition, the interaction of functional groups with surface defects, e.g., steps, may lead to specific adsorption sites, which are favorably occupied at low coverages.<sup>6–8</sup> Finally, we note that the interaction of the functional groups with the surface is also decisive for the lateral diffusion of the molecules on dielectric surfaces.<sup>9</sup>

For the system studied in this work, namely, perylene-3,4,9,10-tetracarboxyl acid dianhydride (PTCDA) on the KCl(100) surface,<sup>10,11</sup> a commensurate long-range ordered

monolayer has been found, like-wise to the situation on the NaCl(100) surface.<sup>12,13</sup> Concerning the commensurability of the structures, this system bears similarity to PTCDA on the low index Ag surfaces,<sup>1</sup> although the interfacial bonding is of different type. On PTCDA negative charge is localized on the two anhydride groups, in particular on the four carboxylic O atoms (see Figure 1).

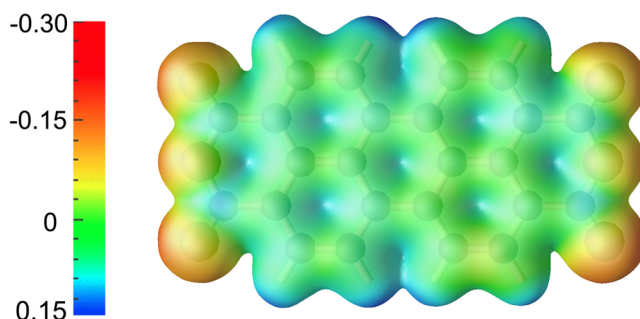


**Figure 1.** Calculated local electrostatic potential of the PTCDA molecule (in eV) shown along the charge density isosurface  $0.1 \text{ e}/\text{Å}^3$ . Red/blue regions indicate low/high values of the electrostatic potential.

**Received:** September 24, 2014

**Revised:** November 19, 2014

**Published:** November 20, 2014

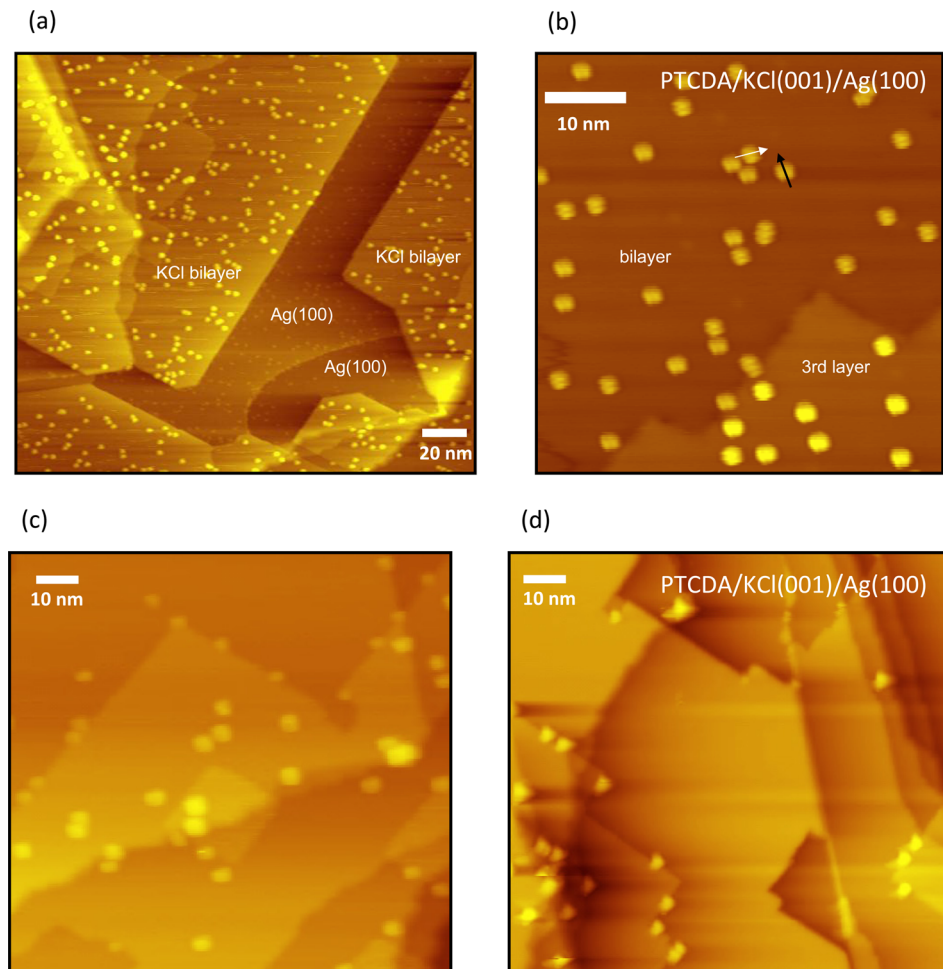


**Figure 2.** (a) Overview of isolated PTCDA molecules deposited at about 100 K on a KCl film of about 3 ML thickness on average ( $190.2 \text{ nm} \times 209.0 \text{ nm}$ ). The nominal coverage is about 1% of a full monolayer. The image was recorded at cryostat temperature of 12 K ( $U_{\text{bias}} = -2.1 \text{ V}$ ;  $I = 113 \text{ pA}$ ). The PTCDA molecules are found to be statistically distributed on the terraces. (b) STM image of a smaller area ( $53.9 \text{ nm} \times 52.2 \text{ nm}$ ,  $U_{\text{bias}} = 2.5 \text{ V}$ ;  $I = 83 \text{ pA}$ ) with high resolution. Note that only PTCDA molecules with azimuthal orientations of the long axis along the two polar  $\langle 011 \rangle$  orientations can be observed. (c,d) Two STM images ( $99.7 \text{ nm} \times 104.9 \text{ nm}$ ) after the first (c) annealing cycle at 150 K, and the second additional postannealing at 200 K (d) for about 10 min. These images demonstrate that annealing causes the terraces to empty and the molecules migrate to step edge sites ( $U_{\text{bias}} = -1.5 \text{ V}$  (c) and  $-1.4 \text{ V}$  (d); and  $I = 58 \text{ pA}$  (c) and  $59 \text{ pA}$  (d)).

PTCDA adsorbed on KCl(100) forms a long-range ordered commensurate monolayer with a brick-wall structure, which is different from the lateral packing that is favored by pure intermolecular interactions.<sup>10,11</sup> PTCDA on the NaCl(100) surface behaves similarly.<sup>12,13</sup> From density-functional theory (DFT) it was concluded that in the favored adsorption configuration the molecular center is on top of a Cl<sup>-</sup> anion, and the four carboxylic oxygen atoms are close to surface cations, i.e., the K<sup>+</sup> ions, hence anchoring the molecule on its four corners on the surface by attractive Coulomb interactions.<sup>14,15</sup>

An interesting situation arises if very small quantities of PTCDA molecules are deposited and can interact with surface defects, in particular with steps. This aspect was first studied by Karacuban et al. for PTCDA deposited on the NaCl(100).<sup>16</sup> They reported that PTCDA molecules adsorb preferably at the defective  $\langle 100 \rangle$  oriented step edge. In particular, they identified a so-called “vacancy site” as most stable. This result was recently confirmed by some of the present authors by performing density functional theory (DFT) calculations.<sup>15</sup> The adsorption at a step-edge vacancy or kink site was found to be energetically preferred by 1.22 or 0.49 eV, respectively, compared to adsorption at flat terraces. Previous fluorescence

spectroscopy experiments<sup>17</sup> suggested a similar scenario for PTCDA on KCl(100) surfaces. In order to explore and rationalize the PTCDA adsorption on KCl(100) in detail, the present study combines low-temperature scanning tunneling microscopy (STM) with DFT calculations. It is found that PTCDA preferentially adsorbs at KCl surface step sites. In particular, an energetically very favorable “deep vacancy site” is identified, which appears to be created by the diffusion of KCl molecules along the steps.

## 2. METHODOLOGY

**2.1. Experimental Section.** The experiments have been performed under ultrahigh vacuum in a two chamber apparatus. The base pressure was  $2 \times 10^{-10} \text{ mbar}$ . One chamber was equipped with a variable temperature scanning tunneling microscope (STM) manufactured by RHK technology, the other was used for KCl film preparation and PTCDA deposition. The STM can be operated with the sample being cooled by a liquid He cryostat. The cryostat is at  $\sim 12 \text{ K}$  and the sample temperature, which cannot be measured precisely at low temperature, is reckoned to be below 40 K. The STM tip was made from Pt–Ir. Given bias voltages ( $U_{\text{bias}}$ ) refer to the

voltage at sample with respect to the tip. All STM images shown here were recorded in constant current mode.

In the preparation chamber, the sample was cooled by liquid nitrogen and the lowest temperature during PTCDA deposition was  $\sim 100$  K. The Ag(100) surface was prepared by the cycles of sputtering with 700 eV Ar<sup>+</sup> ions and annealing at 820 K. Thin epitaxial KCl films were then grown on the Ag(100) substrate at a rate of 0.2 atomic layers per min, while the sample was at temperatures between 300 and 450 K. KCl was thermally sublimated from a boron-nitride crucible. Details of the preparation of the KCl films are reported in ref 11. We find that KCl grows on Ag(100) in the form of a wetting layer consisting of two atomic layers (bilayer), on top of which layers of monatomic height nucleate. This is in contrast to what we erroneously concluded from our earlier STM experiments<sup>11</sup> and will be reported elsewhere. This type of growth scenario seems to be typical for many alkali halides.<sup>18</sup> PTCDA was deposited from a Knudsen cell onto the KCl films at a sample temperature of 100 or 300 K. After the deposition at 100 K, the sample was transferred into the STM chamber as fast as possible and cooled down there below 40 K.

**2.2. Computational Section.** The calculations have been performed using the Vienna Ab Initio Simulation Package (VASP) implementation<sup>19</sup> of DFT. The PW91 functional<sup>20</sup> is used to model the electron exchange and correlation interaction within the generalized gradient approximation (GGA). The electron–ion interaction is described by the projector-augmented wave (PAW) method.<sup>21</sup> Plane waves up to an energy cutoff of 400 eV are used as basis functions. Dispersive interactions play an important role for systems such as studied here and may contribute substantially to the surface adsorption energy of organic molecules. Therefore, we complemented the DFT total energy by an additional London-type correction<sup>22</sup> in order to account for dispersive forces in a numerically affordable way. This so-called DFT-D approach has been shown to yield remarkably reliable results for a variety of adsorbate systems, see, e.g., refs 23–25. The sampling of the Brillouin zone was done using a (2  $\times$  2  $\times$  1)  $k$ -point grid. This ensures that the numerical error bar that arises from the Brillouin zone integration is less than 1 meV for relative adsorption energies. In all calculations, convergence criteria of  $10^{-5}$  eV for the total energy and a convergence criterion of 0.03 eV/Å for the maximum final force were used. The repeated-slab method with a vacuum layer of 40 Å was used to simulate the surfaces. If not stated otherwise, six atomic KCl layers were used to model the substrate. This thickness of the material slab has been found to lead to relative adsorption energies that are numerically converged within 1 meV. The atoms in the two lowest layers were kept frozen at ideal bulk positions during structure optimization. The remaining substrate atoms as well as the adsorbate were allowed to relax freely. The same setup was used to model the step edges in a sawtooth-like model system<sup>15</sup> with terraces wide enough to suppress interaction between periodic images of the molecule or the step itself. Adsorption energies are calculated as

$$E_{\text{ads}} = E_{\text{sys}} - E_{\text{sur}} - E_{\text{mol}}$$

where  $E_{\text{sys}}$  is the energy of the adsystem, while  $E_{\text{sur}}$  and  $E_{\text{mol}}$  are the energies of the clean substrate and the energy of the molecule in the gas phase, respectively.

### 3. RESULTS AND DISCUSSION

**3.1. Adsorption on Terraces at Low Temperatures.** An overview STM image is shown in Figure 2a. The local thickness of the KCl film varies. The central part of the image shows two terraces of the bare Ag(100) surface, separated by a monatomic step. They are limited by KCl bilayers, i.e., terraces of KCl consisting of two atomic layers, which can be identified from straight edges in the nonpolar ⟨100⟩ orientation. Further layers of KCl are separated by monatomic steps, which are also mainly oriented along the ⟨100⟩ orientation. Earlier theoretical simulations already<sup>26</sup> predicted the ⟨100⟩ NaCl step edges to be significantly more stable than ⟨111⟩ steps at all accessible values of the chlorine chemical potentials. The same result apparently holds for KCl.

**3.1.1. Lateral Diffusion.** The STM image was recorded after about 1% of a full monolayer of PTCDA<sup>11</sup> had been deposited onto the sample at  $\sim 100$  K, transferred into the STM chamber and cooled down below 40 K.

For these preparation conditions, we find the molecules to be adsorbed statistically on the surface. There are no signs for a preferential adsorption of the PTCDA molecules at step edges. This indicates the lateral diffusion to be very small at temperatures below 100 K and that the molecules hit and stick during the deposition process. We determine the lateral diffusion barriers of PTCDA on KCl(100) by calculating the potential energy surface (PES). Thereby, the molecular adsorption energies are laterally sampled on a dense mesh with a distance of 0.1 Å between the grid points, taking the molecular center as reference. The long axis of the molecule is kept parallel to the ⟨110⟩ orientation of the surface by constraining the lateral degrees of freedom of two inner carbon atoms, which are restricted in their motion to the z direction. All other atoms are allowed to relax freely. The resulting energy landscape is shown in Figure 3. The calculations predict a maximum corrugation of 0.87 eV for the PES and diffusion barriers of 0.58 eV. Single PTCDA molecules on flat KCl(100) surfaces in the minimum energy configuration (adsorption energy  $-2.49$  eV) adsorb with the carboxyl oxygen atoms on top of surface cations, while the molecular center is on top of a surface anion. The carboxyl (anhydride) oxygen atoms of the molecule are 0.4 (0.17) Å closer to the surface than the center of the molecule. The distance between the carboxyl oxygen atoms of the molecule and the surface cations beneath is 2.76 Å, while the distance between the center of the molecule and the surface anion beneath is 3.40 Å. The surface cations beneath the carboxyl oxygen atoms are pulled out of the surface by 0.13 Å, and the surface anions underneath the molecular perylene rings are pushed into the substrate due to a repulsive interaction, cf. ref 15. The configuration where the carboxyl oxygen atoms are above surface anions and the center of the molecule is above a surface cation, in contrast, is energetically most unfavorable. The repulsion between the carboxyl oxygen atoms of the molecule and the surface anions beneath lead to an upward shift of the carboxyl oxygen atoms in this configuration.

**3.1.2. STM Contrast.** An STM image of the same layer but with higher magnification is shown in Figure 2b. Interestingly, all molecules are imaged with a coffee bean-like shape. We found this type of STM contrast at positive and negative bias voltages and explain this by the fact that at a significant tip to sample distance the tip mainly images the lowest unoccupied (LUMO) or the highest occupied molecular orbital (HOMO)

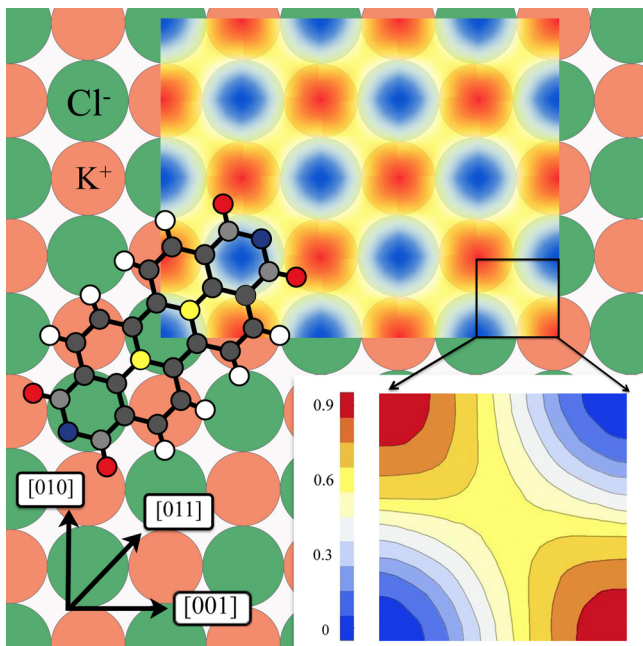


**Figure 3.** Calculated potential energy surface (PES) of PTCDA on KCl(100). The energetically most favored structure corresponds to energy zero (in eV), with positive energies for less favorable adsorption configurations. The inner two atoms, indicated in yellow, were laterally fixed for the PES calculation. See text for details.

of the molecule. The large distance causes submolecular resolution of the orbitals to be absent, and only the node plane along the long molecular axis of the PTCDA is imaged in both situations, yielding the coffee bean-like shape. Notably, this type of STM contrast was also observed for PTCDA deposited on KBr films on InSb.<sup>27</sup> Important in the context of the present results is that all molecules are oriented with their long axis exclusively along two directions with a relative angle of 90° to each other. This is illustrated by the two molecules marked with arrows on the right-hand side of the image. The corresponding directions are the [011] and [0̄11] directions, which define the ⟨011⟩ orientation. This is the polar orientation that is rotated by 45° with respect to the nonpolar ⟨001⟩ orientation. The latter could be experimentally identified from the preferential direction of the straight nonpolar KCl step edges, which are oriented along the ⟨100⟩ orientation as described in ref 11.

**3.1.3. Rotational Barriers.** We have calculated the adsorption energy as a function of the molecular rotation angle in order to rationalize the molecular orientation, see Figure 4. The experimentally observed 45° orientation with respect to the substrate ⟨001⟩ orientation indeed corresponds to the global energy minimum. The adsorption configuration with the molecular axis parallel to ⟨001⟩ represents a local energy minimum. An activation energy of less than 0.15 eV is required only to reach the favorable 45° orientation. This explains the experimental observation that the azimuthal ordering is present already at 100 K, while the lateral mobility of the molecules (to be activated by at least 0.58 eV) is still very limited at this temperature. Similar findings were already reported by Mohn et al.<sup>14</sup> for PTCDA molecules adsorbed on NaCl films. We mention that the ⟨011⟩ azimuthal orientation of the molecules on KCl(100) after deposition at low temperatures observed here has also been concluded from polarized fluorescence experiments.<sup>17</sup>

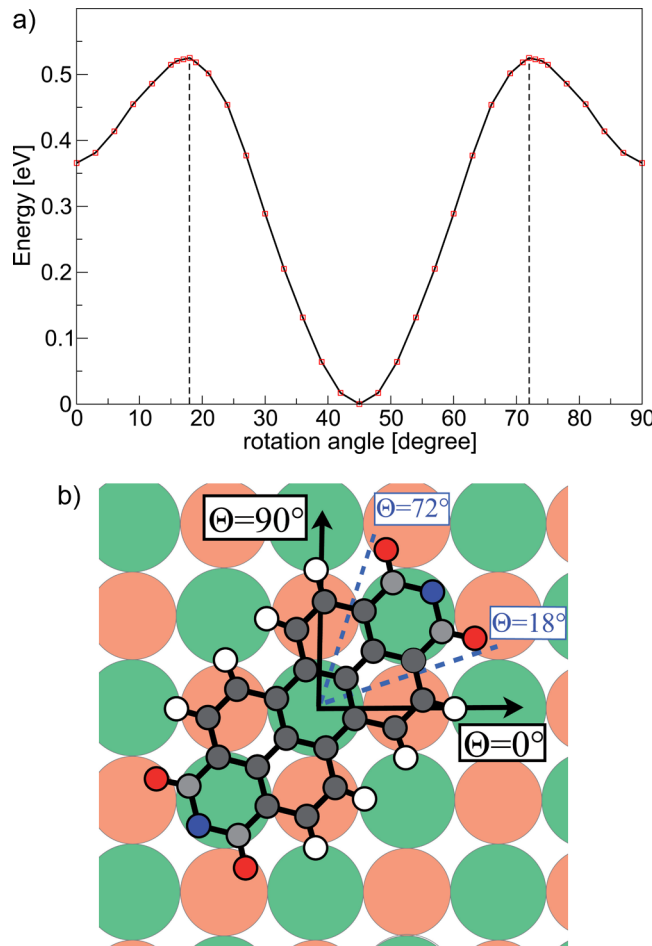


**Figure 4.** Hardsphere model (a) and calculated energies (b) as a function of the rotational angle of a single PTCDA molecule adsorbed on KCl(001). The angle  $\Theta$  is defined as the angle between the long molecular axis and the substrate [001] direction, i.e., the  $\Theta = 0^\circ$  direction. The energy of the molecule in the energetically most favored orientation ( $\Theta = 45^\circ$ ) corresponds to energy zero. The diagram illustrates the rotational barriers for the molecule.

Figures 2c,d displays two STM images recorded after the sample has been subject to additional annealing cycles after the deposition of PTCDA molecules onto the cold sample (100 K). After the sample was annealed to 150 K for 10 min, the molecules start to decorate the step edges, while there are still many molecules on the terraces (Figure 2c). After the second annealing cycle at 200 K for 10 min (Figure 2d) the PTCDA molecules are exclusively found at the step edges. This reveals that adsorption at the step edge sites is thermodynamically favored and that adsorption on the terrace sites is only kinetically stabilized. Obviously, a sufficient lateral diffusion is present above 150 K, which allows the PTCDA molecules to diffuse to the energetically more stable step-edge sites. A similar result was deduced earlier from fluorescence spectroscopy on this system.<sup>17</sup> However, there it was found that sufficient lateral diffusion was already present at ~70 K. We suppose that the difference could be related to the fact that the films used for the STM experiments were of smaller thickness (<5 atomic layers) compared to those used for the optical experiments (~10 layers).

**3.1.4. Role of the Film Thickness for Diffusion.** In order to explore the reason for this apparent change of the diffusion

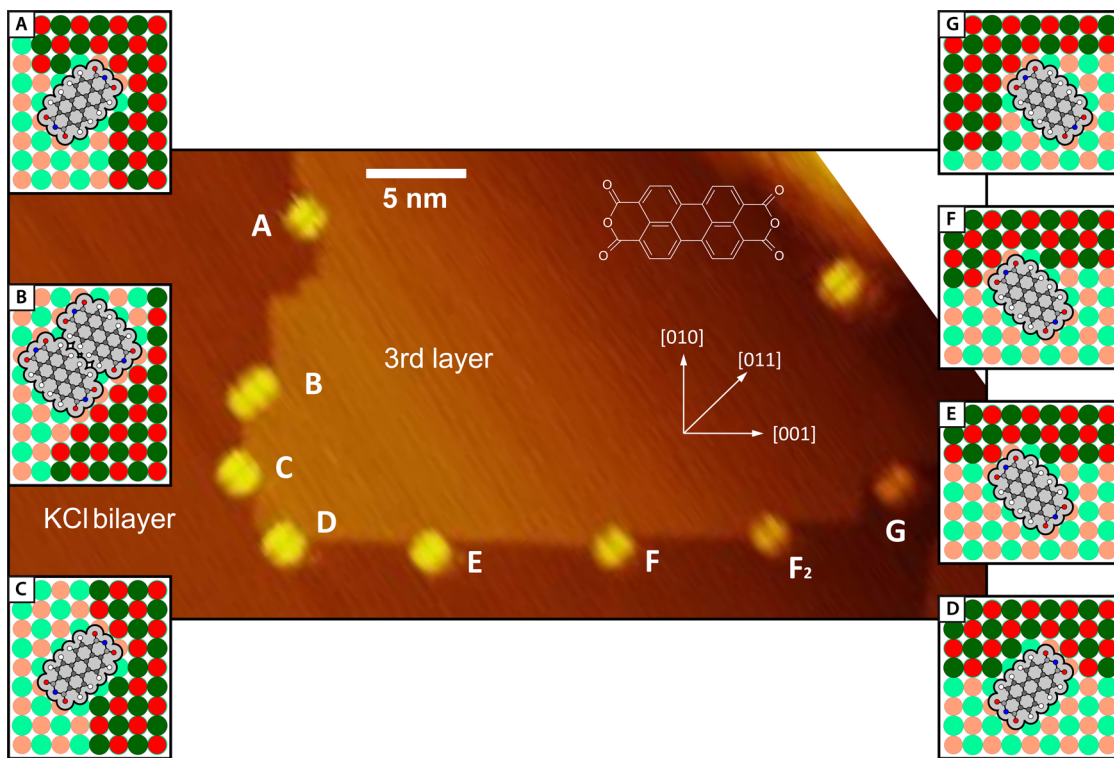


**Figure 5.** STM image of PTCDA molecules adsorbed at different adsorption sites at the step edges of an KCl island on the KCl bilayer on Ag(100) ( $22.7 \text{ nm} \times 46.6 \text{ nm}$ ;  $U_{\text{bias}} = -1.0 \text{ V}$  and  $I = 95 \text{ pA}$ ). Deposition and imaging were both performed at room temperature. Note the image was rotated for clarity and that the scan direction is at about an angle of  $45^\circ$ . The insets show hard sphere models of the different adsorption sites. In addition, the structure formula of PTCDA is given.

barriers, additional calculations were performed. Decreasing or increasing the thickness slab to two or eight atomic layers, respectively, did not modify the diffusion barriers measurably. This indicates that the experimentally observed change of the diffusion barriers is not a direct result of the different film thicknesses. However, two additional factors conceivably affect the diffusion barriers: the change of the KCl lattice constant and the inclusion of Ag(100) layers beneath the bilayer KCl film. Indeed, we find a distinct influence of the KCl lattice constant on the diffusion barrier: The compression/expansion of the KCl lattice constant by about 5% reduces/increases the calculated diffusion barriers by about 0.1/0.04 eV. While this could have an measurable influence if the metal strains the KCl film (as reported, e.g., for NaCl on Cu(111)<sup>28</sup>), one also has to state that no changes of the KCl lattice constant upon epitaxial growth of KCl on Ag(100) have been observed experimentally<sup>11</sup> and that this effect can hence be ruled out. Next, the adsorption of PTCDA on two layers of KCl on top of an Ag(100) substrate was modeled, starting from the structural configuration described in ref 11. In comparison to the calculations for the six layer KCl slab without Ag substrate, we find that the lateral diffusion barriers and surface corrugation are increased from 0.58 and 0.87 eV to 0.77 and 1.14 eV, respectively, while the orientation and the registry of the molecule with respect to the surface do not change, apart from very minor structural modifications that are below 0.03 Å. This agrees with earlier experimental findings.<sup>11</sup> From these calculations we conclude that an electronic rather than a structural effect of the metal substrate modifies the molecular diffusion barriers. The detailed exploration of this effect is beyond the scope of this article. We mention, however, that an

extension of Cu substrate metallic states into the first few layers of a thin NaCl film was proven earlier by Repp et al.<sup>2</sup>

Typically we were able to perform STM measurements on KCl films up to a thickness of about 5 atomic layers, using small tunnel currents in the range below 100 pA and bias voltages in range of +3.5 to -2.0 V. Concerning the contrast of the PTCDA molecules we made the observation that molecules adsorbed on areas of the KCl film that are locally thicker (in terms of atomic KCl layers) appear brighter and larger than those on the bilayer. This can be seen for instance by careful inspection of Figure 2b. There the molecules on the third layer of KCl in the lower left corner appear brighter than those on the KCl bilayer in the upper part of the image. This may possibly be traced again to substrate metallic states, which extend through the KCl film. These states are increasingly suppressed for increasing KCl thickness. This is expected to lead to a relative enhancement of the PTCDA wave function with respect to the bare KCl surface. Correspondingly, the tip retraction on PTCDA molecules in constant current mode becomes more pronounced for thicker KCl films. This effect is reproduced in our DFT simulations of STM images (not shown here). Mohn et al. suggested that PTCDA adsorbed on a NaCl bilayer on Cu(111) is charged by electron transfer from the Cu substrate.<sup>14</sup> This suggestion is not supported by the present observations: Charged molecules will repel each other rather than form pairs with small distances. Such pairs, however, occur frequently, as can be seen in Figure 2.

**3.2. Adsorption at Step Sites. 3.2.1. Different Adsorption Sites.** An STM image with high resolution is shown in Figure 5. It was recorded after PTCDA was deposited on the KCl film at room temperature. Hence the preparation of this sample was different to that discussed above. Nevertheless, we expect that

the final configurations of the molecules at the steps are the same in both cases. Different adsorption configurations of PTCDA at the step edges can be identified in Figure 5. They are denoted by A to G.

All molecules at step edges have their long axes parallel to the  $\langle 011 \rangle$  orientation, as found before for the molecules on the terrace sites. This observation was also made by polarized fluorescence spectroscopy.<sup>17</sup> Since this technique averages over a large number of molecules, this agreement strongly suggests that the configurations seen in STM image can be considered as representative. None of the adsorption sites in Figure 5 correspond to a simple nonpolar step-edge site, a Cl-terminated step-edge, or a kink site (see Figure 6). Instead, it appears as if

to lower the adsorption energy with respect to the terrace site, by at least 0.08 eV.

This high adsorption energy of the vacancy site was proven previously for NaCl step edges.<sup>15</sup> However, the energy gain with respect to molecular adsorption on flat terraces is smaller on KCl (0.79 eV) than for NaCl (1.22 eV). This may result from the smaller lattice constant of NaCl compared to KCl, which leads to smaller vacancies. This, in turn, increases the interaction between molecular oxygen and vacancy Na atoms as well as between the molecular hydrogen and vacancy Cl atoms: For the case of KCl and NaCl, the respective O–Cl distances are calculated to be 4.8 and 4.0 Å.

The adsorption energy increases further when the vacancy site has larger facets of positively charged K atoms, which interact with the oxygen atoms of the molecule, and larger Cl-terminated facets, which attract the hydrogen atoms of the molecule. This case is denoted as “deep vacancy site” (see Figure 7). The deep vacancy sites resemble the simple vacancy site. However, three K–Cl pairs must dissociate from the step-edge in order to realize it. Thereby, the molecule is deeper embedded into the step edge. The adsorption energy of the molecule at this site amounts to  $-3.75$  eV, which is far more favorable than for flat terraces. We tentatively assign the sites C and D in Figure 5 to the deep vacancy site, while E may correspond to a vacancy site. This assignment is supported by the finding that the molecule in D confirmation is deeper embedded into the step-edge compared to site E, while the steps outside of these sites are still straight. The other configurations highlighted in Figure 5, i.e., sites A, B, F, and G, do not have straight steps on the both sides of the molecule. On site F ( $F_2$ ), it looks like one additional row (two additional rows) of  $K^+$  and  $Cl^-$  ions forms along the retracted part of the vacancy site. Accordingly, we denoted these sites as vacancy site + 1 (vacancy site + 2). The molecule at site A is deeply embedded into the step-edge with extra  $K^+$  and  $Cl^-$  ions. Figure 7 gives an overview of hard sphere models for the different plausible sites. On these sites, our calculations reveal the molecule to have adsorption energies of  $-3.44$ ,  $-3.47$ , and  $-3.76$  eV at a vacancy site + 1, vacancy site + 2, and a deep-vacancy + 1 site, cf. Table 2.

**3.2.2. Formation of the Adsorption Sites.** How does the PTCDA adsorption at the step defects, e.g., at a vacancy site, occur? Obviously different kinetic pathways can be thought of. Molecules may diffuse on the surface until they are trapped by a two atom wide vacancy at a step edge. However, given the comparatively large formation energy of step-edge vacancies (cf. Table 2), this scenario appears unlikely. It is more probable that the molecules adsorb at a step-edge kink site first, and then an additional row of  $K^+$  and  $Cl^-$  ions forms along the retracted part of the step edge part by KCl molecules diffusing on the surface. This latter possibility is also suggested from the observation of the sites F and  $F_2$  (cf. Figure 5), which we denote “vacancy site + 1”. This type of site is obtained from the vacancy site in the same way; namely, by adding one additional row of ions on one side of the molecule. Hence we have strong indications that surface KCl diffusion is important for the formation of these sites. We note that diffusion of KCl molecules instead of single ions is plausible because, as reported by Hove,<sup>29</sup> the heat of sublimation of KCl is 2.2 eV and hence far smaller than the dissociation energy of KCl pairs. The vacancy site formation directly upon molecular adsorption at the step edge is another possibility. In order to probe this computationally, we calculated the defect formation energies of

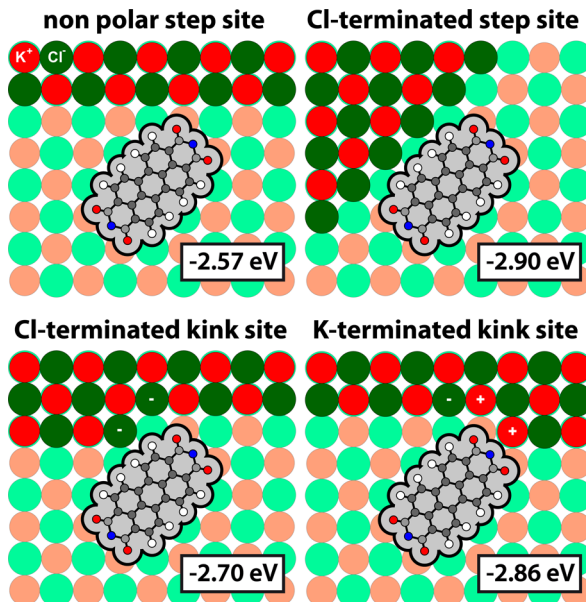
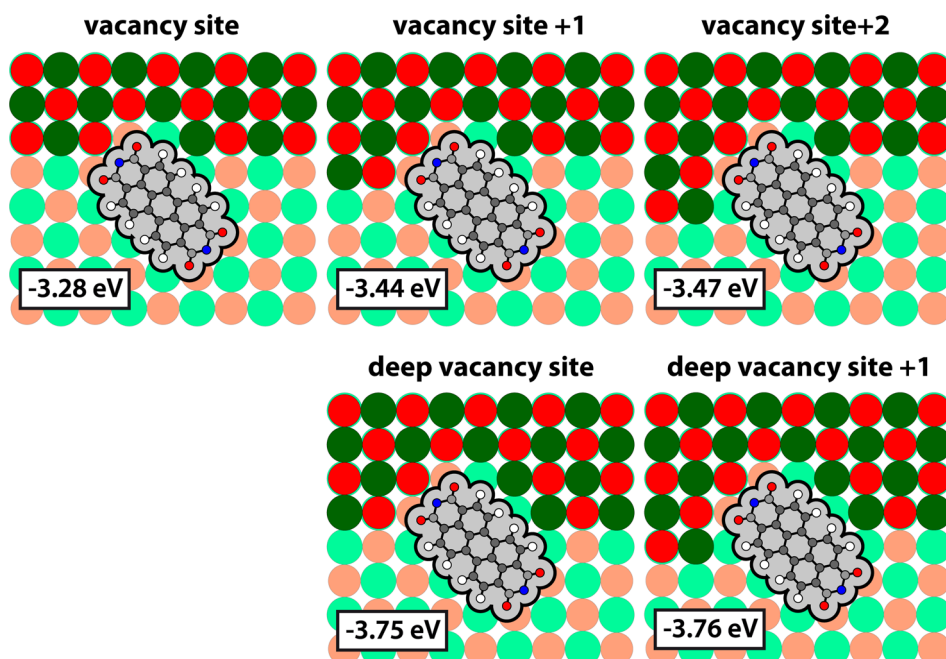


Figure 6. Overview on hard sphere models and DFT calculated adsorption energies of various possible adsorption sites of PTCDA at KCl step edges.

all the PTCDA molecules have partially been embedded into the KCl island, i.e., the molecules exclusively adsorb at vacancies of the step edge. The vacancy site E in Figure 5 is the simplest of those. As mentioned above, this type of site was already found for step-edge decoration of PTCDA on NaCl layers by Karacuban et al.<sup>16</sup> Although we cannot identify the polarity of the ions from our STM image, it appears plausible that the cations ( $K^+$ ) face the negatively charged anhydride groups of the PTCDA and thus lead to attractive interactions of the PTCDA with the step edge ions.

These experimental findings are supported by DFT calculations, which have been performed for a variety of possible molecular adsorption configurations at straight nonpolar and polar steps and at step-edge defects (see Figures 6 and 7 and Tables 1 and 2). For all structures considered the registry of the molecule, with respect to the lower terraces, is similar to that on the flat surface with the orientation of the long axis parallel to the  $\langle 110 \rangle$  orientation. The comparison of the calculated adsorption energies in Tables 1 and 2 shows that the vacancy sites are most favored with respect to the other defect sites or the adsorption on flat terraces. Even the least favorable vacancy adsorption site is 0.42 eV more favorable than the most favored kink site. However, irrespective of the kind of defect, any of the surface defects studied here is found



**Figure 7.** Overview on hard sphere models and DFT calculated adsorption energies of various possible adsorption geometries of PTCDA at different types of vacancy sites at KCl step edges.

**Table 1. Calculated Adsorption Energies of PTCDA at Flat Terraces and at the Adsorption Sites Illustrated in Figure 6**

adsorption site	adsorption energy (eV)
terrace site	-2.49
nonpolar step edge site	-2.57
Cl-terminated polar step edge site	-2.90
Cl-terminated kink site	-2.70
K-terminated kink site	-2.86

**Table 2. Calculated Energies Related to the Adsorption of PTCDA for Different Types of Defect Sites at KCl Step Edges**

adsorption site <sup>a</sup>	adsorption energy (eV)	defect formation energy (eV) <sup>b</sup>	net adsorption energy gain (eV) <sup>c</sup>
vacancy site	-3.28	0.57	-0.22
vacancy site + 1	-3.44	1.28	0.33
vacancy site + 2	-3.47	1.53	0.55
deep vacancy site	-3.75	1.51	0.25
deep vacancy site + 1	-3.76	1.91	0.64

<sup>a</sup>The respective sites are illustrated in Figure 7. <sup>b</sup>Formation energies of the respective defects (without molecules). <sup>c</sup>Net energy gains for molecular adsorption at the respective defects with respect to adsorption on flat terraces.

the step defect configurations (without admolecules) shown in Figure 7. Thereby we calculate the energy differences between the straight steps and the defective steps and assume that the KCl at the steps is in equilibrium with bulk KCl, i.e., it has the same chemical potential. The defect formation energies obtained this way (second column in Table 2) need to be taken into account when comparing the molecular adsorption energies at defective steps, straight steps, and flat terraces. Obviously, even after the vacancy formation energy of 0.57 eV

has been taken into account, there remains a net energy gain of -0.22 eV for molecular adsorption at the vacancy site versus the flat terrace site (third column in Table 2).

The energy gain is reduced to -0.14 eV, but still significant when comparing the molecular adsorption at straight nonpolar step edges with adsorption at vacancy sites. Thus, a molecular adsorption induced defect formation is at least thermodynamically conceivable. The experimental verification of the adsorption mechanism is difficult. The observation that essentially only molecule-occupied step-edge vacancies are found with STM (see Figure 5), however, suggests that these vacancies are indeed formed subsequent to molecular adsorption. Moreover, it appears that the intrinsic kink density on the [100] orientated steps is too small to serve as the only seed points for the formation of the observed density of molecule-occupied vacancy sites, thus supporting the suggested model of a molecular adsorption induced vacancy formation. In fact, at higher coverages we find the molecules to decorate and erode the entire step edge, which is consistent with the scenario that KCl pairs are actively replaced by PTCDA at the step edges. However, the proposed mechanism is thermodynamically favorable only for vacancy sites. The formation energy of all other defects considered here exceeds the energy gain due to molecular adsorption at the defect rather than at the flat terrace, see third column in Table 2. The formation of these adsorption sites thus necessarily occurs kinetically, e.g., by adsorption of KCl molecules diffusing on the terraces at these sites, as described above. In these cases the attractive interaction of the PTCDA with the step edge does not overcompensate the additional line tension caused by the corresponding empty vacancy site.

#### 4. CONCLUSIONS

We have analyzed the adsorption sites of PTCDA on the KCl surface, on terraces, and at step edges. Remarkably, the step edges act as anchoring points for the PTCDA molecules. There we have indications that the formation of vacancy sites by

expelling a KCl molecule is a thermodynamically favored process. As a consequence the formation of and the adsorption at these vacancy sites is always possible and does not require the presence of defects at the step edge ahead. The scenario is analogous to that found for PTCDA on NaCl,<sup>16</sup> and we propose that it may be possibly valid for similar systems, too.

## AUTHOR INFORMATION

### Corresponding Author

\*E-mail: sokolowski@pc.uni-bonn.de.

### Present Address

<sup>†</sup>State Key Laboratory of Magnetic Resonance and Atomic and Molecular Physics, Wuhan Institute of Physics and Mathematics, Chinese Academy of Sciences, Wuhan 430071, P. R. China.

### Notes

The authors declare no competing financial interest.

## ACKNOWLEDGMENTS

We thank Dr. W. Reckien for giving us advice on the shape of the PTCDA orbitals. Financial support from the DFG through SFB 813, SFB 624, SO407/8-1, and the D-A-CH project FWF I958 is gratefully acknowledged. The calculations were done using grants of computer time from the Paderborn Center for Parallel Computing (PC<sup>2</sup>).

## REFERENCES

- (1) Bauer, O.; Mercurio, G.; Willenbockel, M.; Reckien, W.; Schmitz, C. H.; Fiedler, B.; Soubatch, S.; Bredow, T.; Tautz, F. S.; Sokolowski, M. The Role of Functional Groups in Surface Bonding of Planar  $\pi$ -conjugated Molecules. *Phys. Rev. B* **2012**, *86*, 235431–11.
- (2) Repp, J.; Meyer, G.; Stojkovic, S. M.; Gourdon, A.; Joachim, C. Molecules on Insulating Films: Scanning-Tunneling Microscopy Imaging of Individual Molecular Orbitals. *Phys. Rev. Lett.* **2005**, *94*, 026803–4.
- (3) Müller, M.; Paulheim, A.; Marquardt, C.; Sokolowski, M. Spectroscopy of Isolated PTCDA Molecules on the KCl (100) Surface: Vibrational Spectra and Azimuthal Orientation. *J. Chem. Phys.* **2013**, *138*, 064703–8.
- (4) Trevethan, T.; Shluger, A. L. Building Blocks for Molecular Devices: Organic Molecules on the MgO (001) Surface. *J. Phys. Chem. C* **2007**, *111*, 15375–15381.
- (5) Hoff, B.; Gingras, M.; Peresutti, R.; Henry, C. R.; Foster, A. S.; Barth, C. Mechanisms of the Adsorption and Self-Assembly of Molecules with Polarized Functional Groups on Insulating Surfaces. *J. Phys. Chem. C* **2014**, *118*, 14569–14578.
- (6) Rahe, P.; Kittelmann, M.; Neff, J. L.; Nimmrich, M.; Reichling, M.; Maass, P.; Kühnle, A. Tuning Molecular Self-Assembly on Bulk Insulator Surfaces by Anchoring of the Organic Building Blocks. *Adv. Mater.* **25**, 3948–3956.
- (7) Such, B.; Trevethan, T.; Glatzel, T.; Kawai, S.; Zimmerli, L.; Meyer, E.; Shluger, A. L.; Amijs, C. H. M.; de Mendoza, P.; Echavarren, A. M. Functionalized Truxenes: Adsorption and Diffusion of Single Molecules on the KBr(001) Surface. *ACS Nano* **2010**, *4*, 3429–3439.
- (8) Nony, L.; Bocquet, F.; Para, F.; Chérioux, F.; Duverger, E.; Palmino, F.; Luzet, V.; Loppacher, C. Dipole-Driven Self-Organization of Zwitterionic Molecules on Alkali Halide Surfaces. *Beilstein J. Nanotechnol.* **2012**, *3*, 285–293.
- (9) Trevethan, T.; Shluger, A. L. Modeling the Diffusive Motion of Large Organic Molecules on Insulating Surfaces. *J. Phys. Chem. C* **2008**, *112*, 19577–19583.
- (10) Dienel, T.; Loppacher, C.; Mannsfeld, S. C. B.; Forker, R.; Fritz, T. Growth-Mode-Induced Narrowing of Optical Spectra of an Organic Adlayer. *Adv. Mater.* **2008**, *20*, 959–963.
- (11) Müller, M.; Ikonomov, J.; Sokolowski, M. Structure of Epitaxial Layers of KCl on Ag(100). *Surf. Sci.* **2011**, *605*, 1090–1094.
- (12) Burke, S. A.; Ji, W.; Mativetsky, J. M.; Topple, J. M.; Fostner, S.; Gao, H. J.; Guo, H.; Grütter, P. Strain Induced Dewetting of a Molecular System: Bimodal Growth of PTCDA on NaCl. *Phys. Rev. Lett.* **2008**, *100*, 186104–4.
- (13) Le Moal, E.; Müller, M.; Bauer, O.; Sokolowski, M. Stable and Metastable Phases of PTCDA on Epitaxial NaCl Films on Ag(100). *Phys. Rev. B* **2010**, *82*, 045301–9.
- (14) Mohn, F.; Repp, J.; Gross, L.; Meyer, G.; Dyer, M. S.; Persson, M. Reversible Bond Formation in a Gold-Atom-Organic-Molecule Complex as a Molecular Switch. *Phys. Rev. Lett.* **2010**, *105*, 266102–4.
- (15) Aldahhak, H.; Schmidt, W. G.; Rauls, E. Adsorption of PTCDA on NaCl(100) and KCl(100). *Surf. Sci.* **2013**, *617*, 242–248.
- (16) Karacuban, H.; Koch, S.; Fendrich, M.; Wagner, T.; Möller, R. PTCDA on Cu(111) Partially Covered with NaCl. *Nanotechnology* **2011**, *22*, 295305–9.
- (17) Paulheim, A.; Marquardt, C.; Müller, M.; Sokolowski, M. Fluorescence Spectroscopy of PTCDA Molecules on the KCl(100) Surface in the Limit of Low Coverages: Site Selection and Diffusion. *Phys. Chem. Chem. Phys.* **2013**, *15*, 4906–4913.
- (18) Matthaei, F.; Heidorn, S.; Boom, K.; Bertram, C.; Safiei, A.; Henzl, J.; Morgenstern, K. Coulomb Attraction During the Carpet Growth Mode of NaCl. *J. Phys.: Condens. Matter* **2012**, *24*, 354006–6.
- (19) Kresse, G.; Furthmüller, J. Efficiency of Ab-Initio Total Energy Calculations for Metals and Semiconductors Using a Plane-Wave Basis Set. *Comput. Mater. Sci.* **1996**, *6*, 15–50.
- (20) Perdew, J. P.; Chevary, J. A.; Vosko, S. H.; Jackson, K. A.; Pederson, M. R.; Singh, D. J.; Fiolhais, C. Atoms, Molecules, Solids, and Surfaces: Applications of the Generalized Gradient Approximation for Exchange and Correlation. *Phys. Rev. B* **1992**, *46*, 6671–6687.
- (21) Kresse, G.; Joubert, D. From Ultrasoft Pseudopotentials to the Projector Augmented-Wave Method. *Phys. Rev. B* **1999**, *59*, 1758–1775.
- (22) Ortmann, F.; Bechstedt, F.; Schmidt, W. G. Semiempirical van der Waals Correction to the Density Functional Description of Solids and Molecular Structures. *Phys. Rev. B* **2006**, *73*, 205101–10.
- (23) Thierfelder, C.; Witte, M.; Blankenburg, S.; Rauls, E.; Schmidt, W. G. Methane Adsorption on Graphene from First Principles Including Dispersion Interaction. *Surf. Sci.* **2011**, *605*, 746–749.
- (24) McNellis, E. R.; Meyer, J.; Reuter, K. Azobenzene at Coinage Metal Surfaces: Role of Dispersive van der Waals Interactions. *Phys. Rev. B* **2009**, *80*, 205414–10.
- (25) Rauls, E.; Schmidt, W. G.; Pertram, T.; Wandelt, K. Interplay between Metal-Free Phthalocyanine Molecules and Au(110) Substrates. *Surf. Sci.* **2012**, *606*, 1120–1125.
- (26) Li, B.; Michaelides, A.; Scheffler, M. Density Functional Theory Study of Flat and Stepped NaCl(001). *Phys. Rev. B* **2007**, *76*, 075401–11.
- (27) Such, B.; Goryl, G.; Godlewski, S.; Kolodziej, J. J.; Szymonski, M. PTCDA Molecules on a KBr/InSb System: A Low Temperature STM Study. *Nanotechnology* **2008**, *19*, 475705–6.
- (28) Repp, J. Rastertunnelmikroskopie und -Spektroskopie an Adsorbaten auf Metall- und Isolatoroberflächen. Ph.D. Thesis, Freie Universität, Berlin, Germany, 2002.
- (29) Hove, J. E. Surface Adsorption and Migration Energies for KCl. *Phys. Rev.* **1955**, *99*, 430–434.